

Prospects for detection of ultra high frequency gravitational waves from compact binary coalescences with resonant cavities

Aurélien Barrau,¹ Juan García-Bellido,² Thierry Grenet,³ and Killian Martineau¹

¹ *Laboratoire de Physique Subatomique et de Cosmologie, Université Grenoble-Alpes, CNRS/IN2P3
53, avenue des Martyrs, 38026 Grenoble cedex, France*

² *Instituto de Física Teórica UAM/CSIC, Universidad Autónoma de Madrid, Cantoblanco 28049 Madrid, Spain*

³ *Institut Néel, Université Grenoble-Alpes, Grenoble INP, CNRS
25 avenue des Martyrs, BP 166, 38042 Grenoble cedex 9*

(Dated: May 14, 2024)

This article aims at clarifying the situation about astrophysical sources that might be observed with haloscope experiments sensitive to gravitational waves in the 1-10 GHz band. The GrAHal setup is taken as a benchmark. We follow a very pedagogical path so that the full analysis can easily be used by the entire community who might not be familiar with the theoretical framework. Different relevant physical regimes are considered in details and some formulas encountered in the literature are revised. In particular, we carefully take into account the fast drift of the gravitational wave frequency and the relevant experimental timescales. We also relax the usual assumption that only the merging phase should be considered. The distances that can be probed and expected event rates are carefully evaluated, taking into account degeneracies between physical parameters. We show where experimental efforts should be focused to improve the sensitivity and we conclude that any detection in the near future is extremely unlikely.

INTRODUCTION

It is quite extraordinary that gravitational waves above the MHz might, in principle, be observed in the near future [1–7]. This article aims at investigating in details the possible inspiralling binary mergers, taking the GrAHal experiment [8, 9] as a benchmark. We follow a very pedagogical path so that all arguments are made clear to non-specialists. An excellent review of the possible sources can be found in [10] whereas an in-depth investigation of the expected signal is given in [3]. The search for light black holes was, in particular, considered in [11, 12].

The basic idea behind the phenomenon is that a gravitational wave propagating through a static electromagnetic field sources a feeble electromagnetic wave at the frequency of the gravitational wave that might be seen by resonant detectors. Technically, the theoretical framework is well established and is the one of the so-called inverse Gertsenshtein effect [13–16].

Clearly, all conceivable sources in the frequency range considered here are exotic, no signal is expected from any known astrophysical source. In this article, we therefore do not focus on the *a priori* most favoured region of the parameter space – non is actually really favoured – but, the other way round, we try to investigate the entire range of mergers that might, in principle, be discovered. For most of the work, we remain agnostic about the formation mechanisms.

We focus on binary systems of black holes and define carefully the relevant variables. We show that a huge range of masses is *a priori* visible for two reasons. First, because fixing the chirp mass, which enters the evaluation of the strain, does not fix the mass of each object. Second – and more importantly – because, for a given observation frequency, varying the amount time (before coalescence) at which the system is observed changes the relevant masses. This is neglected in most studies.

After discussing in details the range of interest for the astrophysical masses, we investigate the maximum distance at which a specific source can be detected. This obviously depends not only on astrophysical parameters but also on the details of the experimental setup. We insist on introducing different important timescales and on defining relevant regimes that are overlooked in the usual literature although they play a fundamental role. Both the required strain and the maximal distance for detection are carefully studied. Our results strongly differ from the formulas often encountered in similar works, not only in numerical estimates but also in the functional dependence upon physical parameters. This is due to our “integrated” treatment of the full process – from the source to the detector –, making our output directly usable, evading the risk of evaluating things in a somewhat inconsistent way.

For the sake of completeness we also consider less compact systems. This obviously makes the situation even worse. We take this opportunity to underline a common misunderstanding associated with compactness.

Finally, we focus on a realistic experiment – the Grenoble Axion Haloscope (GrAHal) – and show that the orders of magnitude of distances to mergers that can be probed are very small. The resulting numbers of expected events are far from allowing any effective detection in the near future. The GrAHal project [8] is mostly designed to search for axion dark matter, but also believed to be an interesting gravitational wave detector in the ultra high frequency range. It relies on a synergy of know-hows on key aspects of such experiments: high magnetic fields and fluxes, ultra-low temperatures, and very low noise quantum detectors. Although the expected sensitivity is quite impressive, it remains insufficient for realistic astrophysical situations.

It should be underlined that quite similar questions were addressed in the pioneering work [12]. In particular, the emphasis was put on a state-of-the-art description of merger rates. It was concluded that detecting individual mergers with current proposals remains difficult. Our work is however very different as its two main ingredients were not considered in [12]. First, in the present article, we do not focus on the merging only but, the other way round, we investigate the entire parameter space opened by considering earlier stages of the coalescence. This changes the relevant masses at a given frequency by more than 10 orders of magnitude. Second, we take into account the temporal aspects more accurately by considering several regimes that are ignored in [12]. This is not a minor correction and this leads to an estimated sensitivity worsened by several orders of magnitude, therefore drastically changing the expected detection rate, even for systems observed at merging.

OBSERVABLE BLACK HOLE MASSES

When dealing with extremely high frequency gravitational waves, light black holes are obvious candidates. A binary system of stellar mass black holes would merge long before the frequency of the emitted gravitational waves reaches the band of interest for this work. Only low-mass black holes, presumably formed in the early universe, might lead to the desired signal.

Usually, the typical (total) mass M of a system of black holes associated with a given experimental frequency ν is deduced from the innermost stable circular orbit, following from $\nu \sim f_{\text{ISCO}} \propto M^{-1}$. This is reasonable in the sense that this corresponds to a signal with maximum strain. This, however, obviously not only discards a huge portion of the parameter space but also neglects the fact that the system spends a tiny amount of time within the detector bandwidth close to its merging whereas it can generate a long, coherent, signal earlier in the inspiralling process. This is taken into account in this work.

In the following, we assume non-spinning black holes and use the basic circular orbit approximation to fix orders of magnitude. If m_1 and m_2 are the masses of each black hole, the chirp mass is defined by:

$$\mathcal{M}_c = \frac{(m_1 m_2)^{\frac{3}{5}}}{(m_1 + m_2)^{\frac{1}{5}}}. \quad (1)$$

The frequency of gravitational waves emitted at time τ before the merging is given by [17]:

$$f(\tau) = \frac{1}{\pi} \left(\frac{5}{256} \frac{1}{\tau} \right)^{\frac{3}{8}} \left(\frac{G \mathcal{M}_c}{c^3} \right)^{-\frac{5}{8}}. \quad (2)$$

It is immediately clear that fixing $f(\tau) = \nu$ does *not* fix the mass \mathcal{M}_c (the fact that choosing the frequency does not determine the mass non-ambiguously is actually trivial from Kepler's law). The frequency depends on the product $\tau^3 \mathcal{M}_c^5$. When the time τ is increased, systems with smaller masses can lead to gravitational waves at the very same frequency. The price to pay is obviously a decrease in the amplitude of the signal, as the relevant masses are smaller and as the process has to be seen earlier in its evolution. However, the frequency of the system is then drifting more slowly and the relevant integrating time, hence the strain sensitivity, will substantially increase. In addition, as we shall quantify this later, a given chirp mass corresponds to a wide range of masses m_1 and m_2 . It is therefore clear that even at a fixed observation frequency ν , a wide range of masses can, in principle, be probed.

More importantly, we would like to argue that the problem is *not* an optimization one, unless primordial black holes have a very extended and flat mass spectrum, leading to a signal spread over a wide frequency range [18]. We simply do not know where the sources (if any) are and the entire parameter range should therefore be investigated, even if the sensitivity is lower in some regions. There is no point focusing on specific masses or on the physical case maximising the signal as this might very well not correspond to the real World. One should keep in mind that we deal here with exotic objects whose existence and characteristics are only predicted in very specific models.

To go further in the characterisation of the range of accessible black hole masses we need to specify some experimental quantities. The formulas given in this article are generic and can be used for a wide range of apparatus. We have however chosen to also express them as normalized to fiducial values corresponding to the GrAHal experiment, as described in Table I. In this table T_{sys} is a benchmark for the system temperature corresponding to the usual sum of the cavity thermal noise $h\nu (\exp(h\nu/k_B T) - 1)^{-1}$, T being the cavity temperature, of the zero-point fluctuations of the blackbody gas and of the amplifier noise temperature (the dominant term). Thanks to the LNCMI multiconfiguration hybrid magnet [19] the GrAHal project will be able to cover a very wide frequency range for haloscopes. The extreme cases considered here, namely 0.34 GHz and 11.47 GHz, should therefore be enough to deal with all experiments of this type. Basically, the idea is to consider the search for ultra high frequencies gravitational waves as an additional feature of haloscopes, reusing the experimental setups and data. The cavity resonant mode of interest for the search of axions or Axion Like Particles (ALPs) being the TM_{010} mode, the relevant frequency of the experimental setup will from now on be set to $\nu = \nu_{TM_{010}}$. Different values of this frequency for the GrAHal platform, corresponding to different possible setups, are listed in Table I. As discussed in [3], due to the tensor nature of gravitational waves, it would be judicious to investigate the coupling with other resonant modes in the cavity, *e.g.* with modes which exhibit a quadrupolar structure. However, as it will be discussed later in this article, an improvement of that kind would unfortunately not change the main conclusions. Hence, we stick to the usual TM_{010} mode for this analysis, which allows a direct reuse of axionic data and facilitates comparisons with already existing studies.

GrAHal configurations				
$B_{\text{max}}(\text{T})$	Cavity volume (m^3)	Benchmark system noise temperature T_{sys} (K)		$\nu_{TM_{010}}(\text{GHz})$
9	5.01×10^{-1}	0.3		0.34
17.5	3.22×10^{-2}	0.3		0.79
27	1.83×10^{-3}	0.4		2.67
40	1.42×10^{-4}	1.0		6.74
43	4.93×10^{-5}	1.0		11.47

TABLE I. Main possible configurations for GrAHal using the LNCMI hybrid magnet [19].

In Fig.1, the chirp mass is displayed as a function of the time before merging for three of the previous configurations (the two extreme ones and the central one). For a given gravitational waves emission frequency – which means a given orbital frequency – there is a full degeneracy (ignoring for the moment other characteristics of the waves) between \mathcal{M}_c and τ . The chirp mass ranges from $10^{15} \text{g} \sim 10^{-18} M_{\odot}$ to $2 \times 10^{-5} M_{\odot}$ for the $\nu = 0.34$ GHz configuration. The upper limit becomes $2 \times 10^{-6} M_{\odot}$ for the $\nu = 2.67$ GHz, and $5 \times 10^{-7} M_{\odot}$ for the $\nu = 11.47$ GHz configuration. This covers more than 10 orders of magnitude in chirp masses.

For the unfamiliar reader, it might be worth clarifying a possible confusion. From Kepler's law it is obvious that considering higher masses at a given frequency requires to increase the distance between the black holes. Therefore it seems that they should be considered earlier in the inspiralling process, meaning that τ should be higher, conflicting with Fig.1 and Eq.(2) which shows, the other way round, that τ is smaller for higher masses. The reason is simply that the distance depends not only on τ but also on \mathcal{M}_c . Otherwise stated, the heavier black holes are indeed at a larger distance – still for a fixed frequency – one from the other but they actually are *closer* to their merging time ($M \propto r^3$ which, using Eq.(3), leads to $\tau \sim r^{-5}$). At fixed frequency, slightly counter-intuitively, the larger the distance, the smaller the merging time.

The lower bound $M_* \sim 10^{15}$ g simply comes from the evaporation of light black holes through the Hawking mechanism [20]. A black hole with mass $m < M_*$ would have fully evaporated in a time smaller than the age of the Universe. As we are confined to nearby objects, there is no chance to observe far-away lighter black holes. This is a firm limit if we assume that they were formed in the early universe. It might nevertheless make sense to also consider black holes at the Planck mass (that is 20 orders of magnitude less massive than the previously given lower bound)

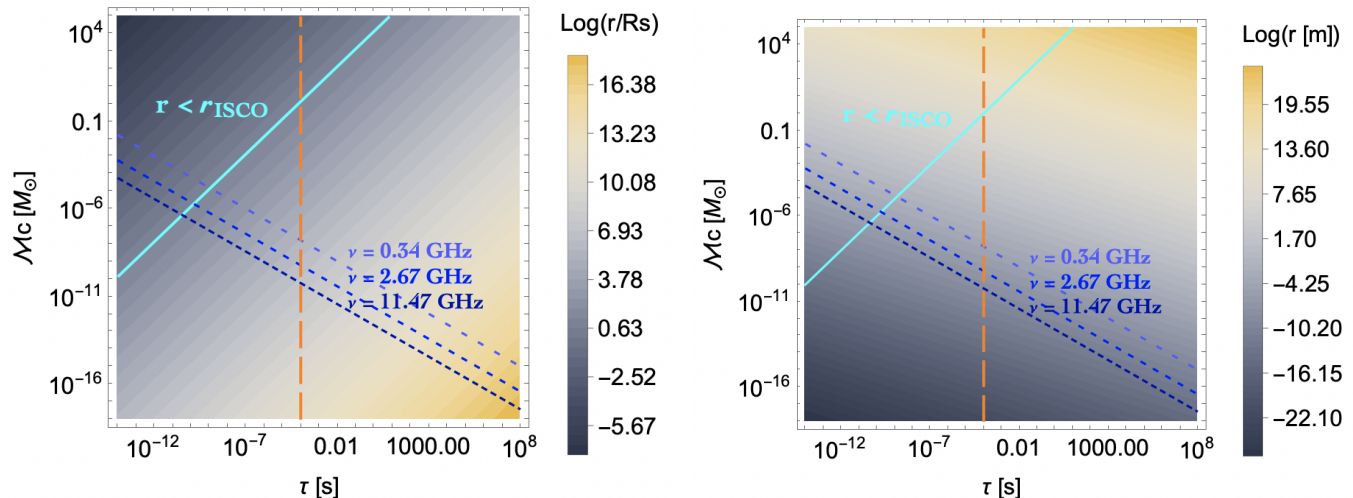


FIG. 1. Left panel: Chirp mass of a binary system of black holes, in solar mass units, as a function of the time before merging for different detector frequencies. The background colors are obtained setting $m_1 = m_2$ and indicate the radial distance between the two bodies in units of their Schwarzschild radius. The slanted cyan line corresponds to this distance being equal to the ISCO radius whereas the vertical orange dashed line corresponds to $\tau = \Delta\nu^{-1}$.

Right panel: Same figure with the radial distance expressed in meters.

as quite a lot of scenarios of quantum gravity (see references in [21]) predict that the evaporation ends with stable relics with masses $m_{rel} \sim M_{Pl} \sim 10^{-5}$ g. This would be an additional point in the plot of Fig. 1 with $\tau \sim 10^{44}$ s (way higher than the age of the universe), for the 2.67 GHz configuration. Obviously, the strain for such gravitational waves is tiny beyond words and this is a purely mathematical situation.

The upper bound corresponds to a pair of black holes reaching their innermost stable circular orbit (ISCO). Basically, it means that the merging is actually taking place: this is the end of the game for the considered system and a single black hole is about to be formed. This limit can be easily evaluated by using the radial distance as a function of the time τ before merging for a quasi-circular orbit [17]:

$$r(\tau) = \left(\frac{256 G^3 M^2 \mu}{5 c^5} \tau \right)^{\frac{1}{4}}, \quad (3)$$

with $M = m_1 + m_2$ and $\mu = m_1 m_2 / (m_1 + m_2)$. Importantly, it should be noticed that r does not depend directly on the chirp mass. However, it is impossible to observe black holes heavier than the mass corresponding to $m_1 = m_2 = 2^{1/5} \mathcal{M}_c^{max}$, where \mathcal{M}_c^{max} is the highest possible chirp mass corresponding to the chosen frequency. It is so because taking a value of m_1 different from m_2 , so that \mathcal{M}_c remains constant, inevitably increases M . As $r_{ISCO} = 6GM/c^2$, the system would have merged.

This deserves a closer look. Once more, it is worth emphasizing that, in principle, the situation is doubly degenerated. For a given detection frequency, there is a huge range of possible chirp masses and, in addition, for each chirp mass \mathcal{M}_c , there is a wide range of allowed individual masses m_1 and m_2 . An obvious lower bound on the m_i 's is M_* (which translates into an upper bound on the other mass). A more subtle upper bound is obtained by the following reasoning. As previously reminded, for a given \mathcal{M}_c , pulling the masses away from $m_1 = m_2$ increases M and therefore the ISCO radius. This is acceptable unless the ISCO radius becomes so large that the associated frequency is now lower than the detection one. In this case the observable frequency is simply never reached in the evolution of the system. This sets an upper limit on the largest mass of the binary system. Figure 2 displays this effect. For every chirp mass compatible with the considered experiment the maximum and minimum individual masses are evaluated. As expected, when the chirp mass approaches the maximum possible one, the system cannot handle a large asymmetry, it would otherwise already be inside its ISCO.

The extreme possible individual masses for a given chirp mass can be analytically calculated, at a fixed detection frequency ν :

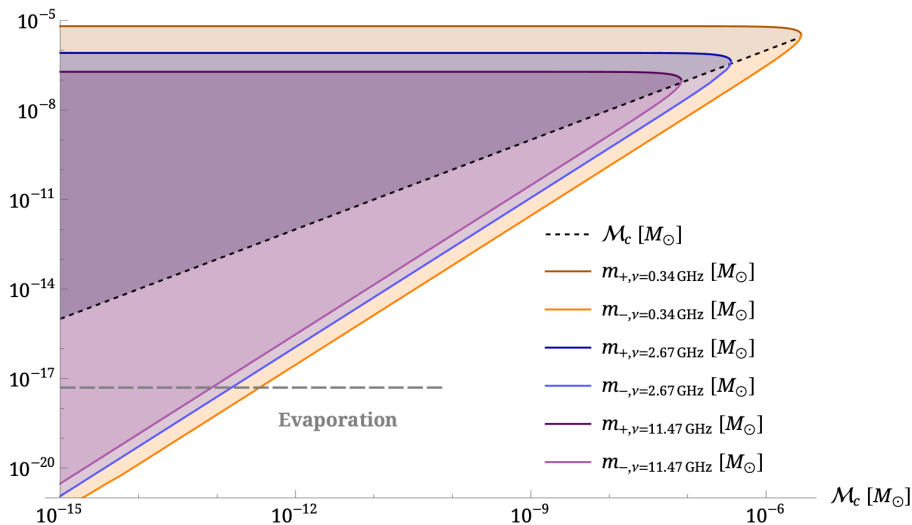


FIG. 2. Minimum and maximum individual masses as a function of the chirp mass, under the constraint that the system has not yet reached its ISCO at the detection frequency.

$$m_{\pm}(\nu, \mathcal{M}_c) = \frac{c^3}{24\sqrt{6}\pi G\nu} \times \left(1 \pm \sqrt{1 - 576\sqrt{3} \times 2^{\frac{1}{6}} \left(\frac{\pi G\nu \mathcal{M}_c}{c^3} \right)^{\frac{5}{6}}} \right). \quad (4)$$

This corresponds to the plain lines on Fig. 2. To summarize: the first figure of this article shows the wide range of chirp masses compatible with a detection configuration whereas the second figure exhibits the wide range of individual masses compatible with each of those chirp masses.

DISTANCES

The post-Newtonian approximation for the strain induced by a source at distance D and detected at frequency ν fixed by the experimental setup reads [17]:

$$h = \frac{2}{D} \left(\frac{G\mathcal{M}_c}{c^2} \right)^{\frac{5}{3}} \left(\frac{\pi\nu}{c} \right)^{\frac{2}{3}}. \quad (5)$$

As is well known, it exhibits a linear dependence on the inverse distance¹. In agreement with intuition, it also increases with the chirp mass and with the frequency, that is, for a given system, when approaching the merging phase. This strain produced by the source is to be compared with the minimum strain detectable by the considered experiment. Following [3], we write the signal power as

$$P_{\text{sig}} = \frac{1}{2\mu_0 c^2} Q (2\pi\nu)^3 V_{\text{cav}}^{\frac{5}{3}} (\eta h B_0)^2, \quad (6)$$

with μ_0 the vacuum magnetic permeability, ν the frequency of the cavity mode TM_{010} , B_0 the magnetic field, Q the quality factor, V_{cav} the cavity volume and η a coupling coefficient characterizing the interaction between the

¹ The energy scales, as usual, as $1/D^2$ but gravitational wave detectors do not “absorb” the signal, hence they see the amplitude and the sensitivity to sources does scale, quite unusually, as $1/D$.

(dimensionless) effective current generated by a gravitational wave inside the cavity and a certain resonant mode, taken to be of order 0.1, as estimated in [3].

Conservative estimate

In order to match with axionic setups and following [3] we estimate the signal-to-noise ratio (SNR) thanks to the Dicke radiometer equation [3, 22, 23],

$$\text{SNR} \sim \frac{P_{sig}}{k_B T_{sys}} \sqrt{\frac{t_{eff}}{\Delta\nu}}, \quad (7)$$

where $\Delta\nu$ is the spectral width, T_{sys} is the system temperature (including all contributions), k_B the Boltzmann constant and t_{eff} is an effective time which depends on the physical situation considered, as will be made clear in the following. It coincides with the integration time only when dealing with systems observed long before their merging.

However, it is not fully established that Eq. (7) gives the final word on the question of the SNR, and a large room for improvement can be expected, especially when considering other detection methods [24]. Nevertheless, we make it our baseline for calculations so as to share a common background with other studies on this topic. As it will be made clear later, it is likely that our conclusions do not depend on the detailed expression used for the SNR.

Requiring $\text{SNR} > 1$ leads to², in the quasi-circular approximation,

$$h > \sqrt{2\mu_0 c^2 k_B} (2\pi\nu)^{-\frac{3}{2}} \eta^{-1} B_0^{-1} V_{cav}^{-\frac{5}{6}} Q^{-\frac{1}{2}} T_{sys}^{\frac{1}{2}} \Delta\nu^{\frac{1}{4}} t_{eff}^{-\frac{1}{4}}. \quad (8)$$

To fix orders of magnitude, we assume that the spectral width entering this calculation is actually the bandwidth of the instrument, that is $\Delta\nu \sim \nu/Q$. This can be debated and this should be investigated in more details in the future – we discuss this point later on. This is however the correct way to go if one relies on the Dicke formula, used consistently with the signal power given by Eq. (6). Normalizing to the three sets of GrAHal fiducial values used for Fig.1, we obtain:

$$\begin{aligned} h &> 4.7 \times 10^{-22} \times \left(\frac{0.34 \text{ GHz}}{\nu}\right)^{\frac{5}{4}} \left(\frac{0.1}{\eta}\right) \left(\frac{9 \text{ T}}{B_0}\right) \left(\frac{5.01 \times 10^{-1} \text{ m}^3}{V_{cav}}\right)^{\frac{5}{6}} \left(\frac{10^5}{Q}\right)^{\frac{3}{4}} \left(\frac{T_{sys}}{0.3 \text{ K}}\right)^{\frac{1}{2}} \left(\frac{1 \text{ s}}{t_{eff}}\right)^{\frac{1}{4}} \\ \Leftrightarrow h &> 1.5 \times 10^{-21} \times \left(\frac{2.67 \text{ GHz}}{\nu}\right)^{\frac{5}{4}} \left(\frac{0.1}{\eta}\right) \left(\frac{27 \text{ T}}{B_0}\right) \left(\frac{1.83 \times 10^{-3} \text{ m}^3}{V_{cav}}\right)^{\frac{5}{6}} \left(\frac{10^5}{Q}\right)^{\frac{3}{4}} \left(\frac{T_{sys}}{0.4 \text{ K}}\right)^{\frac{1}{2}} \left(\frac{1 \text{ s}}{t_{eff}}\right)^{\frac{1}{4}} \\ \Leftrightarrow h &> 4.8 \times 10^{-21} \times \left(\frac{11.47 \text{ GHz}}{\nu}\right)^{\frac{5}{4}} \left(\frac{0.1}{\eta}\right) \left(\frac{43 \text{ T}}{B_0}\right) \left(\frac{4.93 \times 10^{-5} \text{ m}^3}{V_{cav}}\right)^{\frac{5}{6}} \left(\frac{10^5}{Q}\right)^{\frac{3}{4}} \left(\frac{T_{sys}}{1.0 \text{ K}}\right)^{\frac{1}{2}} \left(\frac{1 \text{ s}}{t_{eff}}\right)^{\frac{1}{4}}. \end{aligned} \quad (9)$$

Of course, those formulas are exactly the same ones. We chose to write 3 times the very same thing so that the orders of magnitude can be immediately obtained for fiducial configurations and unit parameters. This allows a direct and simple comparison with the estimations performed in [3] (taking into account that we normalized to $t_{eff} = 1$ s and not $t_{eff} = 1$ min). However, the choice of the effective time t_{eff} is far from being straightforward and deserves a specific analysis as its expression depends upon the considered case and hides some crucial physical quantities. We will investigate this in details and will not leave it as a free parameter. This is one of the key-points of this study.

To this aim, we introduce the duration of the signal within the experimental bandwidth $\Delta\nu$, that is $t_{\Delta\nu} \sim \Delta\nu/\dot{f}(\nu) = \nu/(Q\dot{f}(\nu))$ where

$$\dot{f}(\nu) = \frac{96}{5} \pi^{\frac{8}{3}} \left(\frac{GM_c}{c^3}\right)^{\frac{5}{3}} \nu^{\frac{11}{3}}, \quad (10)$$

² In practice, it might of course be necessary to increase the SNR beyond unity. This is straightforward to implement from our analysis and this would not change the conclusion.

is the time derivative of the emitted gravitational wave frequency taken at the experimental frequency. This leads to

$$t_{\Delta\nu} \sim \frac{5}{96} \pi^{-\frac{8}{5}} \nu^{-\frac{8}{5}} Q^{-1} \left(\frac{G\mathcal{M}_c}{c^3} \right)^{-\frac{3}{5}}. \quad (11)$$

The value of $t_{\Delta\nu}$ as a function of the chirp mass is shown on Fig. 3. The upper “deep” orange zone corresponds to $t_{\Delta\nu} > t_{\max} \sim 1$ year, that is longer than the full duration of the experiment whereas the upper “light” orange zone corresponds to $t_{\Delta\nu} > t_{\max} \sim 60$ s. They are extreme cases for the maximum time (respectively for the full data taking and for a single run). The lower brown zone corresponds to a time spent by the astrophysical signal in the bandwidth smaller than the inverse of the sampling frequency of the experiment, that is $t_{\Delta\nu} < t_{\min} \sim Q/\nu$, as it will be explained in more details later on. Clearly, the dependence of the time spent by the signal within the instrument bandwidth upon the chirp mass is not weak and cannot be ignored.

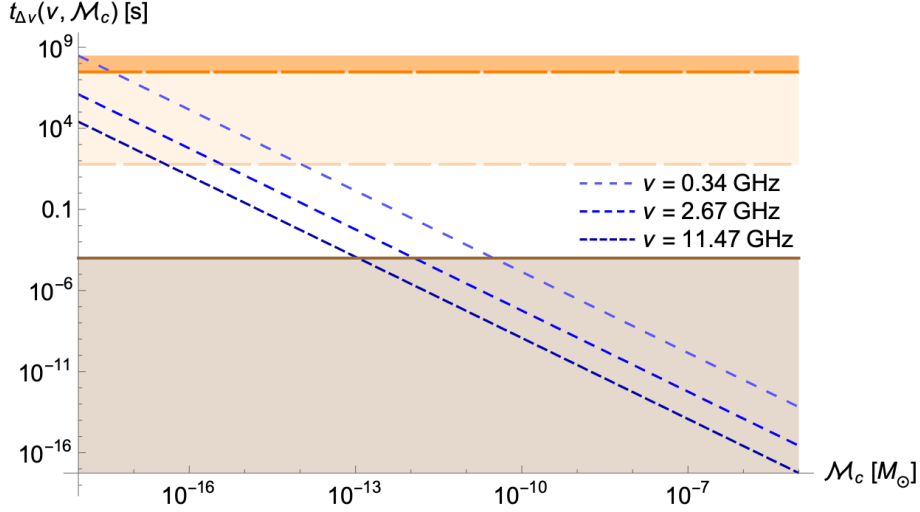


FIG. 3. Time spent by the physical signal within the experimental bandwidth as a function of the chirp mass, for the three frequencies of interest. Upper dashed horizontal line: limit corresponding to an integration time of one year. Middle dashed horizontal line: limit corresponding to an integration time of one minute. Lower plain horizontal line: limit corresponding to $t_{\min} \sim \Delta\nu^{-1} \sim 10^{-4}$ s.

It is important to emphasize that a naive use of the formulas given, *e.g.*, in the reference article [3] might lead to integrate during 1 minute – taken as the fiducial time-scale for the experimental setup – a signal whose real physical duration is less than a nanosecond! This is why the time analyses performed here is mandatory in deriving realistic estimates. The chirp mass is *not* independent of the possible integration time.

Effective time given by the signal frequency drift

This case corresponds to $t_{\min} < t_{\Delta\nu} < t_{\max}$. It means that the effective time entering the calculation of the SNR is the duration of the signal within the frequency bandwidth of the cavity. The associated range of masses is $\mathcal{M}_c \in [\mathcal{M}_{\min}^{\Delta\nu}, \mathcal{M}_{\max}^{\Delta\nu}]$, with:

$$\begin{aligned} \mathcal{M}_{\min}^{\Delta\nu} &= \left(\frac{5}{96} \right)^{\frac{3}{5}} \pi^{-\frac{8}{5}} c^3 G^{-1} \nu^{-\frac{8}{5}} Q^{-\frac{3}{5}} t_{\max}^{-\frac{3}{5}} \\ &= 3.9 \times 10^{-16} \times \left(\frac{2.67 \text{ GHz}}{\nu} \right)^{\frac{8}{5}} \left(\frac{10^5}{Q} \right)^{\frac{3}{5}} \left(\frac{60 \text{ s}}{t_{\max}} \right)^{\frac{3}{5}} M_{\odot}, \end{aligned} \quad (12)$$

and

$$\begin{aligned}
\mathcal{M}_{\max}^{\Delta\nu} &= \left(\frac{5}{96}\right)^{\frac{3}{5}} \pi^{-\frac{8}{5}} c^3 G^{-1} \nu^{-\frac{8}{5}} Q^{-\frac{3}{5}} t_{\min}^{-\frac{3}{5}} \\
&= 2.0 \times 10^{-12} \times \left(\frac{2.67 \text{ GHz}}{\nu}\right)^{\frac{3}{5}} \left(\frac{10^5}{Q}\right)^{\frac{3}{5}} \left(\frac{3.7 \times 10^{-5} \text{ s}}{t_{\min}}\right)^{\frac{3}{5}} M_{\odot}.
\end{aligned} \tag{13}$$

As it will be discussed in the last section of this study, one should notice that t_{\min} actually depends upon Q and ν .

In this situation, $t_{\text{eff}} = t_{\Delta\nu}$ and Eq. (11) can be used directly. Requiring $SNR > 1$ leads to

$$\begin{aligned}
h &> \left(\frac{6}{5}\right)^{\frac{1}{4}} \pi^{-\frac{5}{6}} \mu_0^{\frac{1}{2}} k_B^{\frac{1}{2}} c^{-\frac{1}{4}} G^{\frac{5}{12}} \nu^{-\frac{7}{12}} \eta^{-1} B_0^{-1} V_{\text{cav}}^{-\frac{5}{6}} Q^{-\frac{1}{2}} T_{\text{sys}}^{\frac{1}{2}} \mathcal{M}_c^{\frac{5}{12}} \\
\Leftrightarrow h &> 2.0 \times 10^{-21} \times \left(\frac{2.67 \text{ GHz}}{\nu}\right)^{\frac{7}{12}} \left(\frac{0.1}{\eta}\right) \left(\frac{27 \text{ T}}{B_0}\right) \left(\frac{1.83 \times 10^{-3} \text{ m}^3}{V_{\text{cav}}}\right)^{\frac{5}{6}} \left(\frac{10^5}{Q}\right)^{\frac{1}{2}} \left(\frac{T_{\text{sys}}}{0.4 \text{ K}}\right)^{\frac{1}{2}} \left(\frac{\mathcal{M}_c}{10^{-14} M_{\odot}}\right)^{\frac{5}{12}}.
\end{aligned} \tag{14}$$

For the other setups considered here, the numerical prefactor becomes respectively: 1.6×10^{-22} for the 0.34 GHz configuration and 1.8×10^{-20} for the 11.47 GHz configuration (when taking care to normalize each time the magnetic field, the volume and the temperature to the corresponding proper fiducial values given in table I. This estimate (together with the ones given for the other cases in the following sections) is to be preferred over the proposal of Eq. (9) where correlations between parameters are hidden, leading to misleading feelings about the functional dependencies.

By comparing this requirement with the the signal amplitude given by Eq. (5), it is possible to derive the maximum distance at which the source can be situated to be detected :

$$\begin{aligned}
D &< \left(\frac{40}{3}\right)^{\frac{1}{4}} \pi^{\frac{3}{2}} \mu_0^{-\frac{1}{2}} k_B^{-\frac{1}{2}} c^{-\frac{15}{4}} G^{\frac{5}{4}} \nu^{\frac{5}{4}} \eta B_0 V_{\text{cav}}^{\frac{5}{6}} Q^{\frac{1}{2}} T_{\text{sys}}^{-\frac{1}{2}} (\mathcal{M}_c)^{\frac{5}{4}} \\
\Leftrightarrow D &< 8.1 \times 10^3 \times \left(\frac{\nu}{2.67 \text{ GHz}}\right)^{\frac{5}{4}} \left(\frac{\eta}{0.1}\right) \left(\frac{B_0}{27 \text{ T}}\right) \left(\frac{V_{\text{cav}}}{1.83 \times 10^{-3} \text{ m}^3}\right)^{\frac{5}{6}} \left(\frac{Q}{10^5}\right)^{\frac{1}{2}} \times \left(\frac{0.4 \text{ K}}{T_{\text{sys}}}\right)^{\frac{1}{2}} \left(\frac{\mathcal{M}_c}{10^{-14} M_{\odot}}\right)^{\frac{5}{4}} \text{ m}
\end{aligned} \tag{15}$$

The prefactor for the other setups considered here are: 2.5×10^4 for the 0.34 GHz configuration and 2.5×10^3 for the 11.47 GHz configuration (still normalizing correctly the associated experimental quantities).

Once again, we emphasize that this formula differs from what is usually encountered in the literature (not only because of prefactors but also in the exponents of the physical quantities). This is because it accounts for the fact that the time entering Eq. (16) cannot be set independently of the physical process considered. This is not a small correction but a huge effect. Importantly, the fact that lighter black holes are seen earlier in their in-spiralling history, and therefore spend more time within the detector bandwidth (as the frequency is evolving more slowly), does not counter-balance the decrease in signal intensity. As a result, the mass appears with a positive – and even larger than 1 – power in the distance evaluation.

To fix orders of magnitude, the maximum distance at which a binary system can be detected is $D_{\max} \sim 0.08 \text{ m}$ for the lightest black holes (corresponding to $t_{\max} \sim 1 \text{ yr}$ and black holes of mass $m = 10^{-18} M_{\odot}$) and $D_{\max} \sim 2.3 \text{ AU}$ for the heaviest ones (corresponding to $t_{\min} \sim 0.1 \text{ ms}$ and earth-mass black holes) – one astronomical unit (AU) being of order of 10^{11} m . We shall comment on the numerical values (obviously tiny) in the discussion section as we keep the reasoning formal at this stage. The formula we derive can be used for arbitrary setups.

Effective time limited by the duration of the experiment

This case corresponds to $t_{\Delta\nu} > t_{\max}$. This means that the signal would spend “more time than available” within the cavity bandwidth. This corresponds to very small chirp masses, such that $\mathcal{M}_C < \mathcal{M}_{\min}^{\Delta\nu}$.

For such small masses, the signal is very stable. This is not intrinsic to the considered systems but due to the fact that, the frequency being fixed, the inspiralling process is in this case observed long before the merging. To evaluate the SNR, one must now set $t_{\text{eff}} = t_{\text{max}}$. We, however, keep $\Delta\nu = \nu/Q$. It might, in principle, be possible, in this case, to take advantage of the coherence of the signal. We will however resist the temptation of playing this game as this would spoil the easiness of comparison with other approaches and come at the price of drastically narrowing the probability that the signal falls within the experimental bandwidth. Not to mention that the physical spectral width cannot be *a priori* known as it depends on the unknown chirp mass.

$$h > \frac{1}{2}\pi^{-\frac{3}{2}}\mu_0^{\frac{1}{2}}k_B^{\frac{1}{2}}c\nu^{-\frac{5}{4}}\eta^{-1}B_0^{-1}V_{\text{cav}}^{-\frac{5}{6}}Q^{-\frac{3}{4}}T_{\text{sys}}^{\frac{1}{2}}t_{\text{max}}^{-\frac{1}{4}}, \quad (16)$$

$$\Leftrightarrow h > 5.3 \times 10^{-22} \times \left(\frac{2.67 \text{ GHz}}{\nu}\right)^{\frac{5}{4}} \left(\frac{0.1}{\eta}\right) \left(\frac{27 \text{ T}}{B_0}\right) \left(\frac{1.83 \times 10^{-3} \text{ m}^3}{V_{\text{cav}}}\right)^{\frac{5}{6}} \left(\frac{10^5}{Q}\right)^{\frac{3}{4}} \left(\frac{T_{\text{sys}}}{0.4 \text{ K}}\right)^{\frac{1}{2}} \left(\frac{60 \text{ s}}{t_{\text{max}}}\right)^{\frac{1}{4}}, \quad (17)$$

with prefactors 1.7×10^{-22} for the 0.34 GHz configuration and 1.7×10^{-21} for the 11.47 GHz configuration. Importantly, the minimum required strain does *not* depend on the chirp mass in this case. This is due to fact that the effective duration does indeed not depend upon \mathcal{M}_c .

This leads to:

$$D < 4\pi^{\frac{13}{6}}\mu_0^{-\frac{1}{2}}k_B^{-\frac{1}{2}}c^{-5}G^{\frac{5}{3}}\nu^{\frac{23}{12}}\eta B_0 V_{\text{cav}}^{\frac{5}{6}}Q^{\frac{3}{4}}T_{\text{sys}}^{-\frac{1}{2}}t_{\text{max}}^{\frac{1}{4}}\mathcal{M}_c^{\frac{5}{3}}. \quad (18)$$

$$\Leftrightarrow D < 0.31 \times \left(\frac{\nu}{2.67 \text{ GHz}}\right)^{\frac{23}{12}} \left(\frac{\eta}{0.1}\right) \left(\frac{B_0}{27 \text{ T}}\right) \left(\frac{V_{\text{cav}}}{1.83 \times 10^{-3} \text{ m}^3}\right)^{\frac{5}{6}} \left(\frac{Q}{10^5}\right)^{\frac{3}{4}} \left(\frac{0.4 \text{ K}}{T_{\text{sys}}}\right)^{\frac{1}{2}} \left(\frac{t_{\text{max}}}{60 \text{ s}}\right)^{\frac{1}{4}} \left(\frac{\mathcal{M}_c}{10^{-17}M_{\odot}}\right)^{\frac{5}{3}} \text{ m}.$$

The prefactors for the other setups are: 0.25 for the 0.34 GHz configuration and also 0.25 for the 11.47 GHz configuration. For a haloscope experiment to observe coalescences of so light black holes, the merger would have to take place inside the resonant cavity. Beside the fact that the reasoning applied to compute the signal would clearly break down, this makes no sense. This will be shown in more details in the following sections. Interestingly, from a purely formal point of view, the two extreme configurations lead to the same accessible distance and the 2.67 GHz is the one corresponding to the largest probed volume.

It should be noticed that the chirp mass now enters the maximum distance with an even higher power than in the previous case. This does not come as a surprise as the time integration effect that was playing in the favor of small masses does not play any role in this case.

Obviously, this make the situation even worst than in the previous case, as it is not even possible to take advantage of the full duration of the signal. If one sets $t_{\text{max}} \sim 1 \text{ yr}$ or even the time corresponding to black holes with $m = M_*$, the results will be catastrophic in the entire range covered by this case. (In practice 1 yr is probably not realistic as, for a very long duration, an additional pink noise should be taken into account.) If, however, the maximum integration time is, for experimental reasons, of the order of one minute, this new formula can be used to estimate accurate numbers that might, *a priori* not be fully out of reach.

Effective time limited by the sampling rate

This case corresponds to $t_{\Delta\nu} < t_{\text{min}}$. It means that the time spent by the signal within the experimental bandwidth is so small that it becomes actually smaller than the inverse sampling frequency. This also decreases the naive SNR. It is however an important situation as it corresponds to heavy masses and most of the parameter space. In this case, $t_{\text{eff}} = t_{\Delta\nu}^2/t_{\text{min}}$, where $t_{\Delta\nu}$ is still the actual time spent by the signal in the bandwidth of the detector, given as usual by Eq. (11), and $t_{\text{min}} \sim 1/\nu_{\text{samp}}$ with ν_{samp} the sampling rate chosen at its limit, that it $\nu_{\text{samp}} \sim \Delta\nu \sim \nu/Q$. A higher sampling frequency would not improve the SNR as the cavity acts as a bandpass filter with spectral width $\Delta\nu$. We therefore use $t_{\text{min}} \sim Q/\nu$.

Requiring $SNR > 1$ leads to a minimum strain for detection:

$$\begin{aligned}
h &> \left(\frac{24}{5}\right)^{\frac{1}{2}} \pi^{-\frac{1}{6}} c^{-\frac{3}{2}} G^{\frac{5}{6}} \mu_0^{\frac{1}{2}} k_B^{\frac{1}{2}} \nu^{-\frac{1}{6}} \eta^{-1} B_0^{-1} V_{\text{cav}}^{-\frac{5}{6}} T_{\text{sys}}^{\frac{1}{2}} \mathcal{M}_c^{\frac{5}{6}} \\
\Leftrightarrow h &> 3.3 \times 10^{-18} \times \left(\frac{2.67 \text{ GHz}}{\nu}\right)^{\frac{1}{6}} \left(\frac{0.1}{\eta}\right) \left(\frac{27 \text{ T}}{B_0}\right) \left(\frac{1.83 \times 10^{-3} \text{ m}^3}{V_{\text{cav}}}\right)^{\frac{5}{6}} \left(\frac{T_{\text{sys}}}{0.4 \text{ K}}\right)^{\frac{1}{2}} \left(\frac{\mathcal{M}_c}{10^{-9} M_{\odot}}\right)^{\frac{5}{6}}.
\end{aligned} \tag{19}$$

The values of the prefactors for the other setups are: 1.1×10^{-19} for the 0.34 GHz configuration and 5.2×10^{-17} for the 11.47 GHz configuration.

Even if this case seems to be phenomenologically more interesting because it corresponds to chirp masses $\mathcal{M}_c > \mathcal{M}_{\text{max}}^{\Delta\nu} \sim 10^{-12} M_{\odot}$, we remind the reader that the chirp mass can, anyway, not be too high, otherwise the black holes would be located inside their ISCO (or would even already have merged), as shown on Fig. 1.

In this case the reachable distance is:

$$\begin{aligned}
D &< \sqrt{\frac{5}{6}} \pi^{\frac{5}{6}} c^{-\frac{5}{2}} G^{\frac{5}{6}} \mu_0^{-\frac{1}{2}} k_B^{-\frac{1}{2}} \nu^{\frac{5}{6}} \eta B_0 V_{\text{cav}}^{\frac{5}{6}} T_{\text{sys}}^{-\frac{1}{2}} \mathcal{M}_c^{\frac{5}{6}} \\
\Leftrightarrow D &< 1.1 \times 10^9 \times \left(\frac{\nu}{2.67 \text{ GHz}}\right)^{\frac{5}{6}} \left(\frac{\eta}{0.1}\right) \left(\frac{B_0}{27 \text{ T}}\right) \left(\frac{V_{\text{cav}}}{1.83 \times 10^{-3} \text{ m}^3}\right)^{\frac{5}{6}} \left(\frac{0.4 \text{ K}}{T_{\text{sys}}}\right)^{\frac{1}{2}} \left(\frac{\mathcal{M}_c}{10^{-9} M_{\odot}}\right)^{\frac{5}{6}} \text{ m}.
\end{aligned} \tag{20}$$

The values for the other setups are: 8.1×10^9 for the 0.34 GHz configuration and 1.8×10^8 for the 11.47 GHz configuration.

Lock-in amplifier – monochromatic sources

Let us now consider the case corresponding to a sufficiently monochromatic source, detected by a phase-sensitive instrument such as a lock-in amplifier. In the SNR formula, the bandwidth then has to be taken at the frequency resolution, that is $1/t_{\text{int}}$ [3] where t_{int} is the integration time. The physical criterion for this to be possible is that the frequency drift during the time t_{int} is much smaller than $\Delta\nu$, which reads

$$\dot{f} t_{\text{int}} \ll \frac{\nu}{Q} \Leftrightarrow t_{\text{int}} \ll t_{\Delta\nu}. \tag{21}$$

As expected, this corresponds to the case where the measurement is limited by the duration of the experiment.

The signal to noise ratio now reads [3]:

$$\text{SNR} \sim \frac{P_{\text{sig}}}{k_B T_{\text{sys}}} t_{\text{int}}. \tag{22}$$

This leads to

$$h > \sqrt{2\mu_0 c^2 k_B} (2\pi\nu)^{-\frac{3}{2}} \eta^{-1} B_0^{-1} V_{\text{cav}}^{-\frac{5}{6}} Q^{-\frac{1}{2}} T_{\text{sys}}^{\frac{1}{2}} t_{\text{int}}^{-\frac{1}{2}}, \tag{23}$$

Which translates in

$$D < 4\pi^{\frac{13}{6}} c^{-5} G^{\frac{5}{3}} \mu_0^{-\frac{1}{2}} k_B^{-\frac{1}{2}} \nu^{\frac{13}{6}} \eta B_0 V_{\text{cav}}^{\frac{5}{6}} Q^{\frac{1}{2}} T_{\text{sys}}^{-\frac{1}{2}} \mathcal{M}_c^{\frac{5}{3}} t_{\text{int}}^{\frac{1}{2}}. \tag{24}$$

It should be noticed that the exponents are quite different from those appearing in the previous case, making the functional dependence quite interesting.

Plugging $t_{\text{int}} = (1/100)t_{\Delta\nu}$ leads to

$$h > 4\sqrt{30}\pi^{-\frac{1}{6}}\mu_0^{\frac{1}{2}}k_B^{\frac{1}{2}}c^{-\frac{3}{2}}G^{\frac{5}{6}}\nu^{-\frac{1}{6}}\eta^{-1}B_0^{-1}V_{\text{cav}}^{-\frac{5}{6}}T_{\text{sys}}^{\frac{1}{2}}\mathcal{M}_c^{\frac{5}{6}} \quad (25)$$

$$\Leftrightarrow h > 7.0 \times 10^{-24} \times \left(\frac{2.67 \text{ GHz}}{\nu}\right)^{\frac{1}{6}} \left(\frac{0.1}{\eta}\right) \left(\frac{27 \text{ T}}{B_0}\right) \left(\frac{1.83 \times 10^{-3} \text{ m}^3}{V_{\text{cav}}}\right)^{\frac{5}{6}} \left(\frac{T_{\text{sys}}}{0.4 \text{ K}}\right)^{\frac{1}{2}} \left(\frac{\mathcal{M}_c}{10^{-17} M_\odot}\right)^{\frac{5}{6}},$$

The prefactors are 2.4×10^{-25} for the 0.34 GHz configuration and 1.1×10^{-22} for the 11.47 GHz configuration. The distance is

$$D < \frac{1}{2\sqrt{30}}\mu_0^{-\frac{1}{2}}k_B^{-\frac{1}{2}}\pi^{\frac{5}{6}}G^{\frac{5}{6}}c^{-\frac{5}{2}}\nu^{\frac{5}{6}}\eta B_0 V_{\text{cav}}^{\frac{5}{6}}T_{\text{sys}}^{-\frac{1}{2}}\mathcal{M}_c^{\frac{5}{6}} \quad (26)$$

$$\Leftrightarrow D < 23 \times \left(\frac{\nu}{2.67 \text{ GHz}}\right)^{\frac{5}{6}} \left(\frac{\eta}{0.1}\right) \left(\frac{B_0}{27 \text{ T}}\right) \left(\frac{V_{\text{cav}}}{1.83 \times 10^{-3} \text{ m}^3}\right)^{\frac{5}{6}} \left(\frac{0.4 \text{ K}}{T_{\text{sys}}}\right)^{\frac{1}{2}} \left(\frac{\mathcal{M}_c}{10^{-17} M_\odot}\right)^{\frac{5}{6}} \text{ m}.$$

The prefactors are 1.7×10^2 for the 0.34 GHz configuration and 3.9 for the 11.47 GHz configuration. The quality factor does not anymore enters directly the results.

In practice, a numerical filter might be used in this case to go beyond the $\Delta\nu$ of the cavity. We leave the detailed analysis for a future work.

Summary of the results

Figures 4 and 5 summarize the full study by presenting the strain sensitivity and the maximum distance at which the source can be situated to be detectable as functions of the chirp mass in all the considered regimes. Interestingly, large distances are reached for chirp masses where the instrument is actually *less* sensitive. This is simply because the signal is way more important in this range and this over-compensates the previous effect.

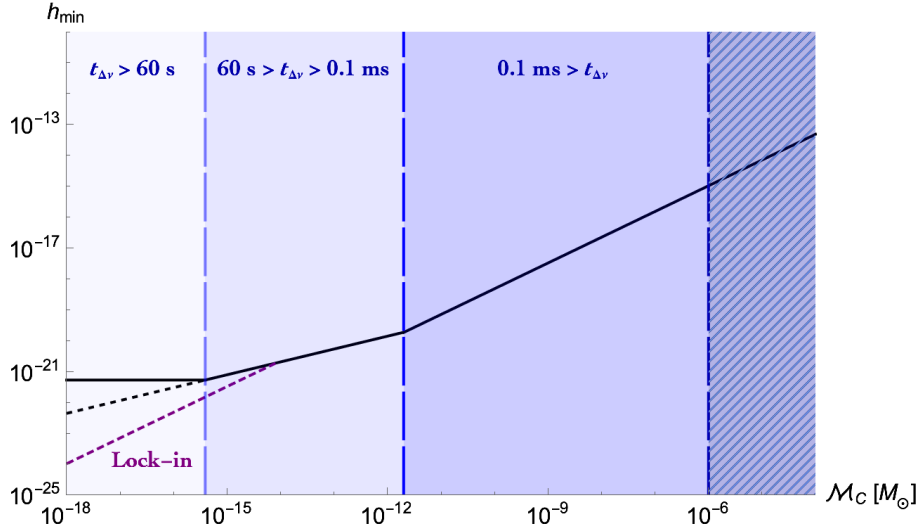


FIG. 4. Strain sensitivity of the GRAHal 2.67 GHz configuration as a function of the chirp mass of the physical system for $t_{\text{max}} = 1$ min. The black dashed line corresponds to $t_{\text{max}} = 1$ year. The purple dashed line corresponds to the lock-in case. The hatched region on the right is excluded by the results presented Fig.1.

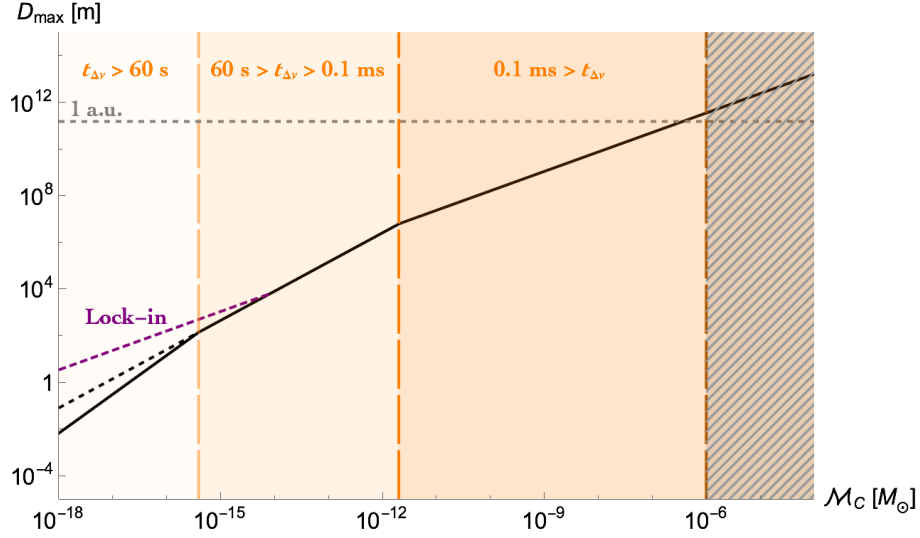


FIG. 5. Maximum distance to the inspiralling system for the GrAHal 2.67 GHz configuration as a function of the chirp mass of the physical system for $t_{\max} = 1$ min. The black dashed line corresponds to $t_{\max} = 1$ year. The purple dashed line corresponds to the lock-in case. The hatched region on the right is excluded by the results presented Fig.1.

EVENT RATE

We now assume that both black holes have the same mass. This is the optimistic scenario. Binaries may form if the black holes were produced very close one to the other so that their dynamics decoupled from the background expansion early enough. This also requires a specific external gravitational influence to prevent the system from directly collapsing. If all the required conditions are met, and assuming that the density of black holes saturates the upper limit derived from microlensing [25], the merging rate can be shown to be [10, 26–28]:

$$\tau \propto \mathcal{M}_c^{-\frac{32}{37}}, \quad (27)$$

or, numerically,

$$\tau \approx 300 \left(\frac{m}{M_\odot} \right)^{-\frac{32}{37}} \text{yr}^{-1} \text{Gpc}^{-3} \quad (28)$$

$$\approx 1.1 \times 10^{-74} \left(\frac{m}{M_\odot} \right)^{-\frac{32}{37}} \text{yr}^{-1} \text{m}^{-3} \quad (29)$$

$$\approx 1.3 \times 10^{11} \left(\frac{m}{10^{-10} M_\odot} \right)^{-\frac{32}{37}} \text{yr}^{-1} \text{Gpc}^{-3} \quad (30)$$

$$\approx 4.8 \times 10^{-66} \left(\frac{m}{10^{-10} M_\odot} \right)^{-\frac{32}{37}} \text{yr}^{-1} \text{m}^{-3}, \quad (31)$$

where $m = m_1 = m_2 = 2^{1/5} \mathcal{M}_c$ (in practice $m \sim \mathcal{M}_c$). The number N of expected events reads $N = 4\pi\tau t_{\text{tot}} D^3/3$ where t_{tot} is the total time of the experimental data taking. This later should not to be confused with the previous time scales entering the different estimates and which were basically corresponding to the sampling time, to the drift duration of the signal in the bandwidth of the experiment, or to the duration of a single “run”. Obviously, Eq. (27) is, in principle, suitable on cosmological scales and a substantial boost factor can be expected when dealing with nearby phenomena. This would however not alter the conclusions.

In the case of an integration time limited by the signal drift, the number of expected events reads:

$$\begin{aligned}
N \approx 1.8 \times 10^{-50} \times & \left(\frac{\nu}{2.67 \text{ GHz}} \right)^{\frac{15}{4}} \left(\frac{\eta}{0.1} \right)^3 \left(\frac{B_0}{27 \text{ T}} \right)^3 \left(\frac{V_{\text{cav}}}{1.83 \times 10^{-3} \text{ m}^3} \right)^{\frac{5}{2}} \left(\frac{Q}{10^5} \right)^{\frac{3}{2}} \\
& \times \left(\frac{0.4 \text{ K}}{T_{\text{sys}}} \right)^{\frac{3}{2}} \left(\frac{m}{10^{-14} M_{\odot}} \right)^{\frac{427}{148}} \left(\frac{t_{\text{tot}}}{1 \text{ yr}} \right).
\end{aligned} \tag{32}$$

The prefactors for the other setups are 5.6×10^{-49} for the 0.34 GHz configuration and 5.2×10^{-52} for the 11.47 GHz configuration. It should first be noticed that the mass appears with the exponent 2.89. The event rate increases very fast with higher masses. This was not *a priori* entirely obvious as 2 different effects do favour small masses. First, as previously explained, the signal spends a longer amount of time within the experimental bandwidth for light black holes. Second, the number density of black holes (and therefore of mergings) per unit time and volume increases – for a fixed total density – for small masses. Still, both those effects are far from compensating the stress increase with large masses.

In the case where the limit is the duration of the experiment (or, more exactly of the “run”) in the previous taxonomy, one is led to:

$$\begin{aligned}
N \approx 3.4 \times 10^{-61} \times & \left(\frac{\nu}{2.67 \text{ GHz}} \right)^{\frac{23}{4}} \left(\frac{\eta}{0.1} \right)^3 \left(\frac{B_0}{27 \text{ T}} \right)^3 \left(\frac{V_{\text{cav}}}{1.83 \times 10^{-3} \text{ m}^3} \right)^{\frac{5}{2}} \left(\frac{Q}{10^5} \right)^{\frac{9}{4}} \\
& \times \left(\frac{0.4 \text{ K}}{T_{\text{sys}}} \right)^{\frac{3}{2}} \left(\frac{m}{10^{-17} M_{\odot}} \right)^{\frac{153}{37}} \left(\frac{t_{\text{max}}}{60 \text{ s}} \right) \left(\frac{t_{\text{tot}}}{1 \text{ yr}} \right).
\end{aligned} \tag{33}$$

The prefactors for the 0.34 GHz and 11.47 GHz setups are respectively equal to 1.7×10^{-61} and 1.8×10^{-61} . As expected, the mass now enters the game with an even higher power of order 4.14. It should also be underlined that two different time scale are in order to estimate the event rate.

In the case where the limit is driven by the sampling rate, the number of events becomes

$$\begin{aligned}
N \approx 2.5 \times 10^{-39} \times & \left(\frac{\nu}{2.67 \text{ GHz}} \right)^{\frac{5}{2}} \left(\frac{\eta}{0.1} \right)^3 \left(\frac{B_0}{27 \text{ T}} \right)^3 \left(\frac{V_{\text{cav}}}{1.83 \times 10^{-3} \text{ m}^3} \right)^{\frac{5}{2}} \\
& \times \left(\frac{0.4 \text{ K}}{T_{\text{sys}}} \right)^{\frac{3}{2}} \left(\frac{m}{10^{-9} M_{\odot}} \right)^{\frac{121}{74}} \left(\frac{t_{\text{tot}}}{1 \text{ yr}} \right).
\end{aligned} \tag{34}$$

The prefactors are 1.0×10^{-36} for the 0.34 GHz configuration and 1.2×10^{-41} for the 11.47 GHz configurations.

The mass dependence is the weakest one, with an exponent close to 1.64. This is directly due to the fact that the positive power entering the maximum distance is smaller, because of the “saturation” effect induced by the limited sampling rate.

Finally, in the case of a phase-sensitive instrument such as a lock-in amplifier the number of event writes:

$$\begin{aligned}
N \approx 2.1 \times 10^{-55} \times & \left(\frac{\nu}{2.67 \text{ GHz}} \right)^{\frac{5}{2}} \left(\frac{\eta}{0.1} \right)^3 \left(\frac{B_0}{27 \text{ T}} \right)^3 \left(\frac{V_{\text{cav}}}{1.83 \times 10^{-3} \text{ m}^3} \right)^{\frac{5}{2}} \\
& \times \left(\frac{0.4 \text{ K}}{T_{\text{sys}}} \right)^{\frac{3}{2}} \left(\frac{m}{10^{-17} M_{\odot}} \right)^{\frac{121}{74}} \left(\frac{t_{\text{tot}}}{1 \text{ yr}} \right).
\end{aligned} \tag{35}$$

The prefactors are 8.6×10^{-53} for the 0.34 GHz configuration and 9.7×10^{-58} for the 11.47 GHz configurations.

The mass dependence is exactly the same than in the previous situation where the limit was driven by the sampling rate.

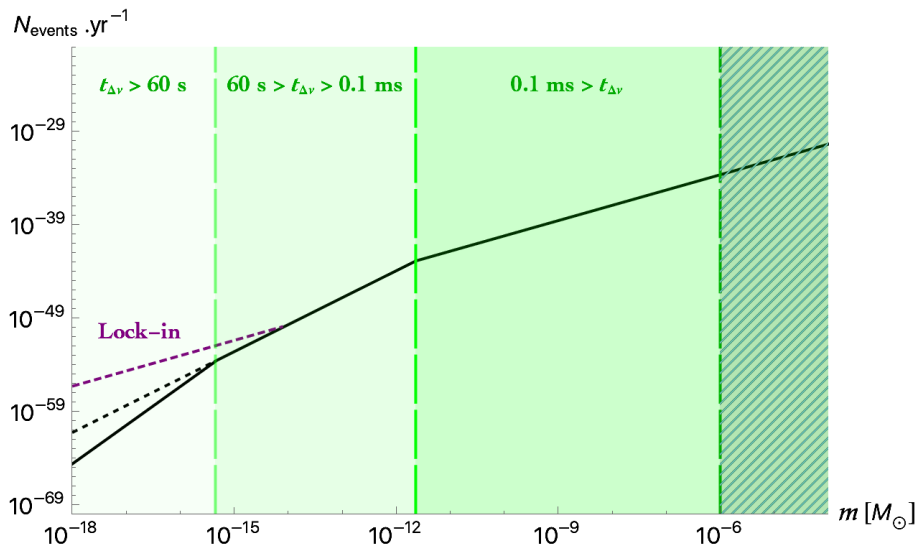


FIG. 6. Number of expected events per year with the GrAHal 2.67 GHz configuration as a function of the black holes mass, assuming that the upper limits on density is saturated. The black dashed line corresponds to an estimate with $t_{\max} = 1$ year whereas the purple dashed line corresponds to the lock-in case. The hatched region on the right is excluded by the results presented Fig. 1.

Figure 6 displays the number of expected events per year for the GrAHal 2.67 GHz configuration. This is a monotonically increasing function of the black hole mass. As expected from the estimations of the distances to mergers, all numerical values are extremely small. Analyses beyond this simple result are performed in the next section.

DISCUSSION

What conclusions can be drawn from the numbers previously obtained? Let us first focus on the event rate.

In the case of the GraHal experiment, for most of the parameter space, the first setup (low frequency range) is the best one and the last setup (high frequency range) is the worst one. This is not so surprising as the usual “figure of merit”, B^2V , often used to have a crude estimate of the performances, is indeed higher when going to bigger volumes (even though the magnetic field is decreased)³. More importantly, one should notice that the way the experimental parameters enter the final estimate does depend on the considered regime – that is on the mass range. This is important to optimize the experimental design. Basically, we show that:

- in all cases, the number of events scales as B_0^3 , $V_{\text{cav}}^{2.5}$, and $T_{\text{sys}}^{-1.5}$,
- for intermediate masses (signal drift limited case), the number of events also scales as $Q^{1.5}$ and $\nu^{3.75}$,
- for small masses (duration of the experiment limited case), the number of events also scales as $Q^{2.25}$ and $\nu^{5.75}$,
- for large masses (sampling rate limited case), the number of events scales as $\nu^{2.5}$ and does not depend on Q .

It might be welcome to increase the dimensionless coupling coefficient η , for example by considering the coupling with other resonant modes in the cavity, as studied in [3]. From the experimental viewpoint it might be the easiest way to increase the sensitivity. However, as η is anyway bounded from above at 1, no dramatic enough improvement can be expected from this side alone.

³ The current haloscopes constraints on the axion-photon coupling follow this trend, see <https://cajohare.github.io/AxionLimits/docs/ap.html>.

In principle, increasing the sampling frequency might seem appealing as it would allow to extrapolate to the region $10^{-12} - 10^{-6} M_{\odot}$ the (more favourable) slope of the curve obtained in the region $10^{-15} - 10^{-12} M_{\odot}$, in Figs. 4, 5, and 6. This is however not possible beyond the value chosen here, which is optimum for a fixed spectral width $\Delta\nu$, that is at given quality factor (once ν is set). Interestingly, for large masses, there is *no* Q-dependence in the calculated sensitivity, distance, and event rates: what is won on the one hand is lost on the other hand. However, the maximal chirp mass $\mathcal{M}_{\max}^{\Delta\nu}$ corresponding to the upper end of the “favourable” regime *does* depend on Q. When inserting the value of t_{\min} saturating the Shannon-Nyquist limit in Eq. (13), one sees that $\mathcal{M}_{\max}^{\Delta\nu} \propto Q^{-6/5}$. This does not come as a surprise as this would increase $\Delta\nu$ and therefore allows for a higher sampling rate. Decreasing Q does however reduce the sensitivity in the intermediate range.

Care should be taken with the ν -dependence as it also changes the maximum (chirp) mass to which the experiment is sensitive. This variable can therefore not be used as naively as the others.

Beyond those scaling laws, the main lesson is that the actual numbers are tiny. We emphasize that no short-run improvement – at least technologically – should raise the event rate near to anything observable. This is one of the main conclusions of this work. Not to mention that several optimistic hypotheses were done. First, it was assumed that the abundance of black holes in the low-mass range correspond to the observed limits, around one percent of the critical density [29]. Moreover, it is also implicitly assumed that most black holes have masses such that the inspiralling signal falls within the (very narrow) experimental bandwidth.

Finally, it should also be reminded, as well known since decades, that the naive extrapolation of the primordial power spectrum observed at large scales, in the cosmological microwave background, leads to a density contrast at small scales which is, by far, too small to produce any black hole. Many smart ways out of this simple conclusion were investigated (see, *e.g.*, [30] and references therein), especially taking into account quantum diffusion in single-field models of inflation [31], leading to a large non-Gaussian exponential tail that enhances the probability of collapse of primordial black holes even for small amplitudes of the power spectrum [32]. However, recent works tend to show that models producing appreciable amounts of primordial black holes generically induce too large one-loop corrections on large scales [33]. This claim has been questioned, particularly in the case of quantum diffusion, but it should anyway be kept in mind that even if the expected event rate was much higher, the way such black holes would be formed would still remain very speculative.

Another point of view could however be advocated: it would consist in not focusing on an “expected” rate but, instead, in investigating which mergers could be detected without violating existing observational constraints, independently of the underlying production mechanism and naively extrapolated cosmological density. By constraints, we mean here direct conflicts with data. The usual limits on the density of primordial black holes indeed rely on the assumption of a smooth distribution following a typical dark matter halo profile. They can be evaded if one assumes a local over-density in the form of PBH clusters, as follows from large non-Gaussian tails [34]. This is however *possible* and phenomenological potentially relevant on this sole basis. A (controversial) argument has even been given to suggest that than some trans-Neptunian anomalies and lensing events might be due to an unexpectedly high amount of local light black holes [35].

However, even this optimistic scenario remains out of reach. Figure 5 indeed shows a kind of conspiracy. Whatever the considered chirp mass, the objects would have to be so close to the Earth (for this mass) that they should already have been detected, either directly or through their gravitational disturbances. Direct detection via *e.g.* X-ray emission from gas falling onto them is however not feasible, due to the extremely low flux received on Earth, even at solar system distances. Planet 9 is an example of gravitational disturbance. We leave a detailed study for a future work.

Clearly, the situation is less dramatic than in the purely consistent dark matter view presented before, and gaining a few orders of magnitude could allow the experiments to reach an interesting sensitivity. The most interesting part is the “high mass” one, that is the one corresponding to the sampling frequency-limited case. As previously shown, at fixed value of ν , the maximum distance for detection scales as $B_0 \times \eta \times V_{vac}^{0.83} \times T^{-0.5}$ and does not depend on Q. This underlines where efforts should be focused and their relative benefits. Of course, for evaluation the possible number of events, one should take the cube of the previous expression but this does not change the relative weights.

Note that we have assumed throughout that the detected gravitational waves come from a circularized orbit of coalescing compact binaries. However, for the small masses we are considering here, the circularization via emission of GW is very inefficient, so one should consider instead highly eccentric orbits [17]. The power emitted by GW in eccentric orbits has an extra factor $F(e) = (1 - e^2)^{-7/2} (1 + 73/24 e^2 + 37/96 e^4)$, so that a very eccentric orbit, with $e \simeq 1$, will emit much more energy per period and thus the connection between strain, distance, masses and

power needs to be reevaluated. We leave for a future publication the analysis of such interesting cases. Very roughly speaking, to be able to efficiently detect those bursts, one would need a strong hierarchy between the orbital frequency of the system and the mean frequency of the emitted gravitational waves, which is not impossible. In this case, one could optimise the detector spectral width just in-between the physically relevant frequencies. This would both allow to have a time sampling of the orbit, therefore taking advantage of the temporal structure of the signal, and to select the resonance frequency at the expected signal frequency. If the signal is spread in Fourier space, much will inevitably be lost.

OTHER SOURCES

Beyond black holes, quite a lot of compact objects could, in principle, be considered. Among other sources, one can think to conventional compact objects, boson stars, fermion stars, dark matter stars, multi-components stars, or dark energy stars [36]. We do not wish to discuss here which ones are compatible with the frequency range considered here and which ones are not. Neither do we investigate the naturalness of those sources. All the relevant models are anyway quite exotic and speculative. We therefore simply discuss briefly the effect of introducing a compactness parameter, in the sense of [37], $C = Gm/(Rc^2)$ – assumed to be the same for the two merging bodies, hence the unspecified mass m and size R for each object.

For black holes, the compactness is $C = 1/2$. It can only be smaller for other sources. This obviously makes the situation even worst. In general, the radius of the innermost stable circular orbit is

$$R_{\text{ISCO}} = \frac{3GM}{C^2}, \quad (36)$$

where, as before, m is the total mass of the considered binary system. As for black holes, the ISCO determines the end of the inspiral phase and the beginning of the merging phase, hence the last stage where the approach considered here basically holds.

It is quite usual in the literature (see, *e.g.* [10]) to express the strain for such a system (assuming that the two objects have the same mass m) as

$$h \propto C \frac{m}{D}. \quad (37)$$

It seems to be proportional to the compactness C . However, in a sense, this way of writing the strain is over-simplistic. The C -factor actually enters this expression of the strain only because (at leading order) it is implicitly written at the ISCO, which is obviously reached earlier for a less compact system. In fact, Eq. (37) gives the maximum strain for a given inspiralling system. This is not the relevant quantity for the analysis presented here as, as explained in the previous sections, the narrow bandwidth of the experiments in the considered frequency range makes it highly unlikely that the system is observed at the most favourable stage of its evolution.

As a consequence, we suggest instead to still consider the results of the previous sections as valid (that is with *no* appearance of the compactness at all in the formulas, even for objects with arbitrary C -factors), but to limit the parameter space to the range where the system has not reached its ISCO. Kepler's law reads

$$\omega_s^2 = G \frac{M}{R^3}. \quad (38)$$

Requiring $R > R_{\text{ISCO}}$, one immediately sees that the maximal mass allowed scales as $C^{3/2}$, namely (remembering that, due to their quadrupolar nature, the frequency of gravitational waves is twice the orbital frequency),

$$M < \frac{c^3}{\pi\sqrt{27}Gf} C^{\frac{3}{2}}. \quad (39)$$

Intuitively, at a given frequency, considering smaller masses requires to have the objects closer one to the other. But, as obvious from Kepler's law, the distance scales as the power 1/3 of the mass. On the other hand, the ISCO radius

scales linearly with the mass. This is why the compactness is an issue for large masses. This basically means that the parameter space previously given simply has to be truncated so that

$$m < \left(\frac{C}{1/2} \right)^{3/2} m_{\max}, \quad (40)$$

where m_{\max} is the maximum allowed individual mass previously estimated. Within this limit (which is stringent for non-compact sources), the previous strain calculation, and therefore the distance estimates, still hold without correcting for the C -factor. One should keep in mind that for most non-exotic objects the ISCO is located inside the considered object!

CONCLUSION

The fact that haloscopes, designed to search for axions, might allow the detection of ultra high frequency gravitational waves is quite amazing. This opens an exciting new window on the Universe. This is obviously a promising and rapidly developing field with appealing features to search for new physics. This might lead to surprises in astrophysics, cosmology, or particle physics.

There might exist interesting stochastic signals, like backgrounds from the early Universe (see references in [10]), detectable by microwave cavities [38]. It could also be that close hyperbolic encounters [39–41] lead to measurable gravitational waves in the frequency band considered here. Several other exotic ideas also deserve consideration. We leave their detailed investigation (among many other possible sources) for future works. In particular, another possibility for detection with these resonant microwave cavities is the redshifted spectrum of GW coming from pre-heating [42, 43]. This spectrum has sufficient amplitude at high frequencies, where there are no expected astrophysical signals, that it is worth exploring.

As far as coherent signals from binary systems – the topic of this work – are concerned it however seems that any detection is very unlikely.

We have performed an in-depth estimate of the sensitivity in all physical regimes and pointed out where experimental improvements would be efficient. We have underlined strong correlations between parameters that are sometimes inappropriately considered as independent and have shown how to take them into account. In particular, temporal aspects have been carefully accounted for. We have calculated distances that can be probed and the related possible rates of events. Current experiments remain very far from the relevant sensitivity.

It would certainly be welcome to investigate in more details the signal-to-noise ratio which has been estimated in an extremely crude way in this work. Although this would, quite certainly, not alter our conclusions, this might be important when dealing with more favourable physical situations. Obviously, a detailed time analysis of the signal would also be important. This should be considered in the future but this study was devoted to the investigation of the way axion haloscopes could be directly used for gravitational waves.

To summarize, the main new inputs of this work – when compared with previous studies – are the following. First, the frequency of the experiment does not fix the mass of the binary systems that could, in principle, be probed: a double degeneracy is at play. Second, and more importantly, the duration of the physical signal in the bandwidth of the instrument can be extremely small and taking this into account drastically reduces the usually assumed sensitivity, hence the number of expected events. This is especially relevant for systems generating the higher strain. Third, for those systems, the limited sampling rate – associated with the fixed bandwidth – does not even allow to measure the signal optimally during this very brief time. This reduces even further the sensitivity.

ACKNOWLEDGEMENTS

JGB acknowledges support from the Research Project PID2021-123012NB-C43 [MICINN-FEDER], and the Centro de Excelencia Severo Ochoa Program CEX2020-001007-S at IFT.

-
- [1] M. Goryachev, W. M. Campbell, I. S. Heng, S. Gallioui, E. N. Ivanov, and M. E. Tobar, Phys. Rev. Lett. **127**, 071102 (2021), 2102.05859.
- [2] M. Goryachev and M. E. Tobar, Phys. Rev. D **90**, 102005 (2014), URL <https://link.aps.org/doi/10.1103/PhysRevD.90.102005>.
- [3] A. Berlin, D. Blas, R. Tito D’Agnolo, S. A. R. Ellis, R. Harnik, Y. Kahn, and J. Schütte-Engel, Phys. Rev. D **105**, 116011 (2022), 2112.11465.
- [4] A. Berlin, D. Blas, R. Tito D’Agnolo, S. A. R. Ellis, R. Harnik, Y. Kahn, J. Schütte-Engel, and M. Wentzel, Phys. Rev. D **108**, 084058 (2023), 2303.01518.
- [5] V. Domcke, C. Garcia-Cely, and N. L. Rodd, Phys. Rev. Lett. **129**, 041101 (2022), 2202.00695.
- [6] V. Domcke and C. Garcia-Cely, Phys. Rev. Lett. **126**, 021104 (2021), 2006.01161.
- [7] N. Herman, A. Füzfa, L. Lehoucq, and S. Clesse, Phys. Rev. D **104**, 023524 (2021), URL <https://link.aps.org/doi/10.1103/PhysRevD.104.023524>.
- [8] T. Grenet, R. Ballou, Q. Basto, K. Martineau, P. Perrier, P. Pugnât, J. Quevillon, N. Roch, and C. Smith (2021), 2110.14406.
- [9] T. Grenet, *The Grenoble Axion Haloscope project*, URL https://indico.cern.ch/event/1119695/contributions/5033901/attachments/2530598/4354011/GrAHal%20project%20FIPs22_v2.pdf.
- [10] N. Aggarwal et al., Living Rev. Rel. **24**, 4 (2021), 2011.12414.
- [11] N. Herman, A. Füzfa, L. Lehoucq, and S. Clesse, Phys. Rev. D **104**, 023524 (2021), 2012.12189.
- [12] G. Franciolini, A. Maharana, and F. Muia, Phys. Rev. D **106**, 103520 (2022), 2205.02153.
- [13] D. Boccaletti, V. De Sabbata, P. Fortini, and C. Gualdi, Nuovo Cim. B **60**, 320 (1969).
- [14] A. Füzfa, Phys. Rev. D **93**, 024014 (2016), 1504.00333.
- [15] A. Füzfa (2017), 1702.06052.
- [16] A. Ejlli, D. Ejlli, A. M. Cruise, G. Pisano, and H. Grote, Eur. Phys. J. C **79**, 1032 (2019), 1908.00232.
- [17] M. Maggiore, *Gravitational Waves. Vol. 1: Theory and Experiments*, Oxford Master Series in Physics (Oxford University Press, 2007), ISBN 978-0-19-857074-5, 978-0-19-852074-0.
- [18] B. Carr, S. Clesse, J. García-Bellido, and F. Kühnel, Phys. Dark Univ. **31**, 100755 (2021), 1906.08217.
- [19] P. Pugnât, R. Barbier, C. Berriaud, R. Berthier, T. Boujet, P. Graffin, C. Grandclément, B. Hervieu, J. Jousset, F. P. Juster, et al., IEEE Transactions on Applied Superconductivity **32**, 1 (2022).
- [20] S. W. Hawking, Commun. Math. Phys. **43**, 199 (1975), [167(1975)].
- [21] A. Barrau, Phys. Lett. B **829**, 137061 (2022), 2201.06988.
- [22] P. Sikivie, Rev. Mod. Phys. **93**, 015004 (2021), 2003.02206.
- [23] A. Berlin et al. (2022), 2203.12714.
- [24] S. K. Lamoreaux, K. A. van Bibber, K. W. Lehnert, and G. Carosi, Phys. Rev. D **88**, 035020 (2013), URL <https://link.aps.org/doi/10.1103/PhysRevD.88.035020>.
- [25] H. Niikura et al., Nature Astron. **3**, 524 (2019), 1701.02151.
- [26] M. Raidal, C. Spethmann, V. Vaskonen, and H. Veermäe, JCAP **02**, 018 (2019), 1812.01930.
- [27] B. Kocsis, T. Suyama, T. Tanaka, and S. Yokoyama, Astrophys. J. **854**, 41 (2018), 1709.09007.
- [28] A. D. Gow, C. T. Byrnes, A. Hall, and J. A. Peacock, JCAP **01**, 031 (2020), 1911.12685.
- [29] H. Niikura, M. Takada, S. Yokoyama, T. Sumi, and S. Masaki, Phys. Rev. D **99**, 083503 (2019), 1901.07120.
- [30] B. Carr and F. Kühnel, Ann. Rev. Nucl. Part. Sci. **70**, 355 (2020), 2006.02838.
- [31] J. M. Ezquiaga, J. García-Bellido, and E. Ruiz Morales, Phys. Lett. B **776**, 345 (2018), 1705.04861.
- [32] J. M. Ezquiaga, J. García-Bellido, and V. Vennin, JCAP **03**, 029 (2020), 1912.05399.
- [33] J. Kristiano and J. Yokoyama (2022), 2211.03395.
- [34] J. M. Ezquiaga, J. García-Bellido, and V. Vennin (2022), 2207.06317.
- [35] J. Scholtz and J. Unwin, Phys. Rev. Lett. **125**, 051103 (2020), 1909.11090.
- [36] G. F. Giudice, M. McCullough, and A. Urbano, JCAP **10**, 001 (2016), 1605.01209.
- [37] A. Alho, J. Natário, P. Pani, and G. Raposo, Phys. Rev. D **106**, L041502 (2022), 2202.00043.
- [38] N. Herman, L. Lehoucq, and A. Füzfa (2022), 2203.15668.
- [39] J. García-Bellido and S. Nesseris, Phys. Dark Univ. **18**, 123 (2017), 1706.02111.
- [40] J. García-Bellido and S. Nesseris, Phys. Dark Univ. **21**, 61 (2018), 1711.09702.
- [41] G. Morrás, J. García-Bellido, and S. Nesseris, Phys. Dark Univ. **35**, 100932 (2022), 2110.08000.
- [42] J. García-Bellido and D. G. Figueroa, Phys. Rev. Lett. **98**, 061302 (2007), astro-ph/0701014.
- [43] J. García-Bellido, D. G. Figueroa, and A. Sastre, Phys. Rev. D **77**, 043517 (2008), 0707.0839.